Transportation and Dispersal of Moss Stems for Terraforming

NASA Colorado Space Grant Consortium DemoSat-B Summer 2022

From left to right: Baylor Jones, Justin Eldridge, Nick Cocetti

Nick Cocetti, Justin Eldridge, Baylor Jones

Colorado State University

Team Moss Boys

8/12/2022

Graduate Advisors: Jacob Gottfried, Anthony (AJ) Puga

CSU NASA Space Grant Director: Dr. Azer Yalin

Table of Contents

Transportation and Dispersal of Moss Stems for Terraforming:

0.0 Acknowledgements

Special thanks to Stacey Anderson who made this all possible through the use of her personal microscopes. Her help with bryophyte research, imaging, and dissection made all of this project possible.

1.0 Introduction

1.1 Goal:

Create a payload to test the effects of near-space conditions on leaf-cell viability in three arctic and antarctic moss species as well as demonstrate the feasibility of a low-altitude dispersal mechanism.

1.2 Mission Statement:

Our mission was to create a payload capable of: exposing moss samples to three distinct near-space environments, protecting an internal compartment from extreme temperatures, and opening said compartment at a specified altitude to drop its contents.

1.3 Introduction

Bryophytes commonly known as moss are an essential first ingredient in the terraforming process because they can inhabit barren rock landscapes in the absence of other vegetation (Longton 1992). Mosses can survive long periods without water (desiccation tolerance) by protecting their cells during dehydration or repairing them on revival (Oliver et al. 2000). Moss can reproduce sexually by forming spores, or asexually by simple fragmentation (Asher 2019). Sexual reproduction is favored for preserving genetic diversity but requires narrow moisture, ph, and temperature ranges which may prove difficult to find. The viability of moss sexual reproduction (through spore germination) has been established for mosses exposed to simulated long-term, low-earth orbit conditions (comparable to terrestrial germination rates)(Takahashi et al. 2011). Meanwhile, asexual fragmenting reproduction is a hardier process with fewer requirements (typically, fragmenting reproduction has a limited dispersal radius because of the surrounding extant plant life, a problem that wouldn't be encountered on barren planetary surfaces)(Lepp 2008).

Here, we examine the viability of moss leaf cells exposed to upper stratospheric conditions. If these cells are in fact viable, they could presumably then undergo asexual fragmentation reproduction, which has not yet been established. We employ the Antarctic moss *Syntrichia ruralis* for its documented ability to survive rapid desiccation and the Arctic moss *Rhytidium rugosum* for its near-exclusive reproduction by fragmentation. The Antarctic moss

Ceratodon purpureus was employed for its ability to change its cells' pigmentation in response to ultraviolet radiation (Post 1990). The complete exposure environment showed an increased number of dead cells relative to the control. The internal environment which was protected from radiation and extremely low temperatures showed the greatest number of dead cells. Upon acquiring the payload after launch, the door mechanism opened during flight and the SD card read data as desired for the flight. The sensor package operated the whole flight and the heating system functioned as intended. The code contained an erroneous "<" symbol which caused the door to open on ascent instead of descent. The door being open may explain the heating system's inability to keep up with dropping temperatures during the flight.

1.4 Mission Importance

The pressures and temperatures found at the edge of space are easily replicated in the lab and incident radiation can be replicated with some difficulty. However, it would be prohibitively difficult and expensive to simulate all these conditions simultaneously. The stratospheric weather balloon represents a cost-efficient and easily replicable method to expose samples. The information gleaned from these experiments will help illuminate the degree of protection these species would need in transit.

2.0 Materials & Methods

2.1 Payload Design

First, for testing the effects of near-space conditions, three onboard testing environments were needed. With these environments in mind, quartz panes were needed to allow as much UV radiation through as possible. Window frames were cut into the insulation and the main structure was altered to accommodate the glass as seen in Figure 1.

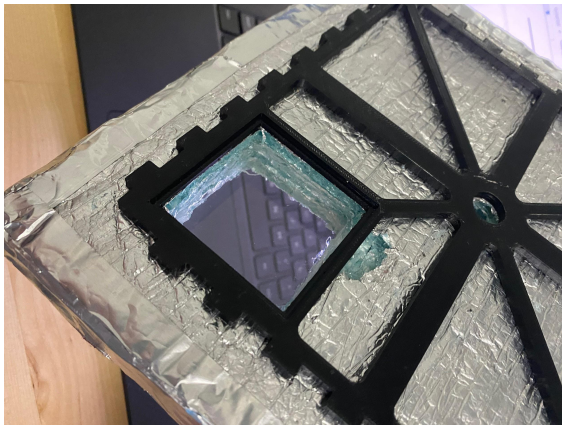

Figure 1: 3D Printed Frame and Quartz Windows

We opted for 3D printing for the main structure of the payload because of its versatility in design. A PETG medium was chosen as it provides a more ductile structure that is better suited for hard impacts such as the drop and stair test. The 3D printed frame provided rigidity and a

mounting surface for the electronics as seen below in Figure 3. The dispersal mechanism was made from PLA (Polylactic Acid) for its resilience to warping. This dispersal mechanism consists of a servo acting as a doorstop, a stepper motor to pull the string, a door housing, and a door with a hole for the string to attach to as seen in Figure 2.

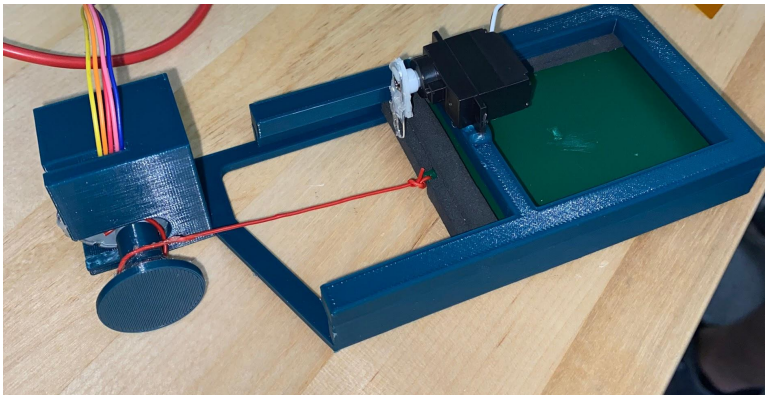

Figure 2: 3D printed dispersal mechanism

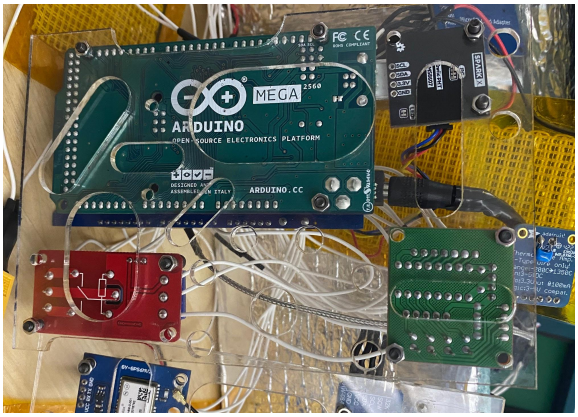

Figure 3: Mounting plate for electronics

The mounting plates were designed in SolidWorks and laser cut to provide high accuracy for hole dimensions and placement. Size #4-40 screws and fasteners were used to secure the electronics to the mounting plates. The mounting plates were then fastened to the 3D-printed frame via zip ties. Extra holes and slots were laser cut into the design to reduce weight as seen in Figure 3.

2.2 Species Selection:

Drought-tolerant mosses from water-scarce environments outperform their cousins when flash-frozen in liquid nitrogen, and are strong candidates for surviving a journey through near space (Burch 2003). After consulting with bryologists Stacey Anderson and Dr. Brent Mishler, we selected Ceratodon purpureus for its pigmentation response to UV radiation; Rhytidium rugosum for its exclusively asexual fragmentary reproduction; and Syntrichia ruralis, for its resilience to rapid desiccation and rapid revival when rehydrated.

2.3 Sample Storage

Candidate moss clumps were photographed, then extracted with a putty knife, and stored in moss packets. The date, time, general location, GPS coordinates, and substrate type were recorded. *Note: the field for species was left blank, pending identification.*

2.4 Sample Identification

We examined samples with a dissecting scope to identify them by their shape, with the help of a bryologist as shown in Figure 4. Species were identified by their leaf shape and cell structures and then confirmed by comparison with New Mexico State University's image archives. The identities of the samples were then recorded.

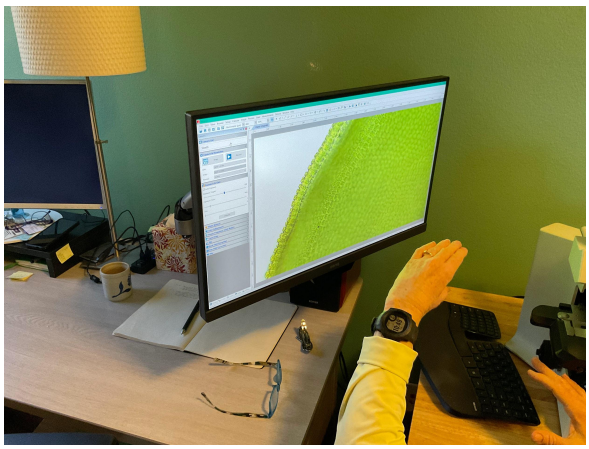

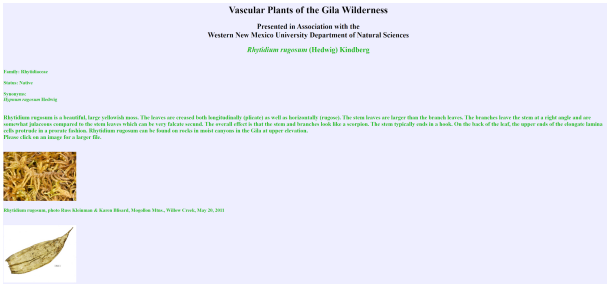

Figure 4: Microscope Inspection and WNM Flora Database

2.5 Sample Storage

The clumps were stored in their packets and placed in a shoebox at room temperature until immediately before launch. The clumps were allowed to dry completely before being manipulated further.

2.6 Sample Imaging

The leaves were photographed at the lowest microscope magnification needed to see cell boundaries. Once a target leaf was centered in the field of view, extended depth focus (EDF) software was employed to compile a single image with the whole leaf in focus (some leaves were large and required composite EDFs to fully capture).

2.7 Transect Lines:

Once the length of a leaf was recorded, five random numbers between one and the length of the leaf were generated. Five perpendicular lines were placed at these distances from the leaf tip as shown in Figure 5. The length of these perpendicular lines was recorded in the datasheet as well. The transect placement was measured using the multipoint curve. Holes in the leaf, folded

portions, and portions otherwise blocked were not included in the length of the transect lines. In the case of holes, another line was placed on the other side of the hole and their two lengths were added together.

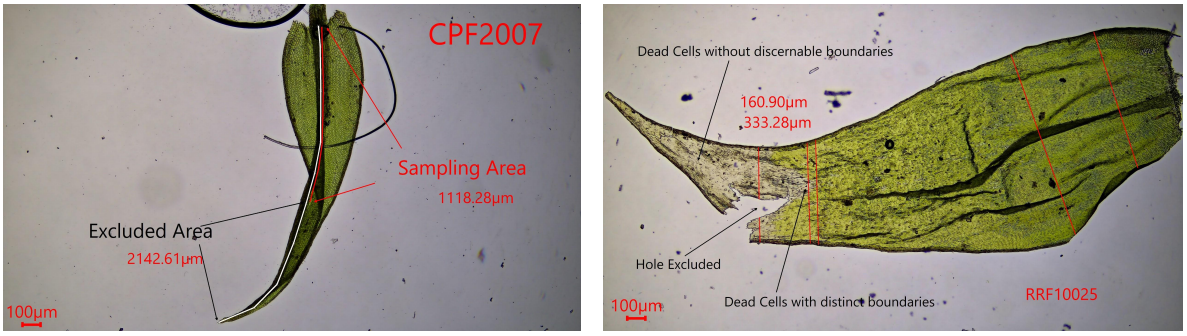

Figure 5: Folded Exclusion Area, Hole Exclusion Area

2.8 Cell Counting

Dead cells, which are colorless and empty, were counted along the transect lines and recorded in the datasheet. Dead cells were identified relative to other cells on the leaf. Some dead cells were distinguishable only by their complete lack of color relative to the rest of the leaf. That is, some cells would be counted as dead when compared to another leaf's healthy cells but counted as alive relative to more obviously dead cells on the same leaf.

As Figure 6 demonstrates, dead patches were difficult to count as the boundaries between cells were often faded or gone completely. In these cases, the average width of medial laminal cells and the width of the dead patch were used to estimate the number of cells within. These widths were taken from Flora of North American Bryophyte datasheets (Rohrer 2014).

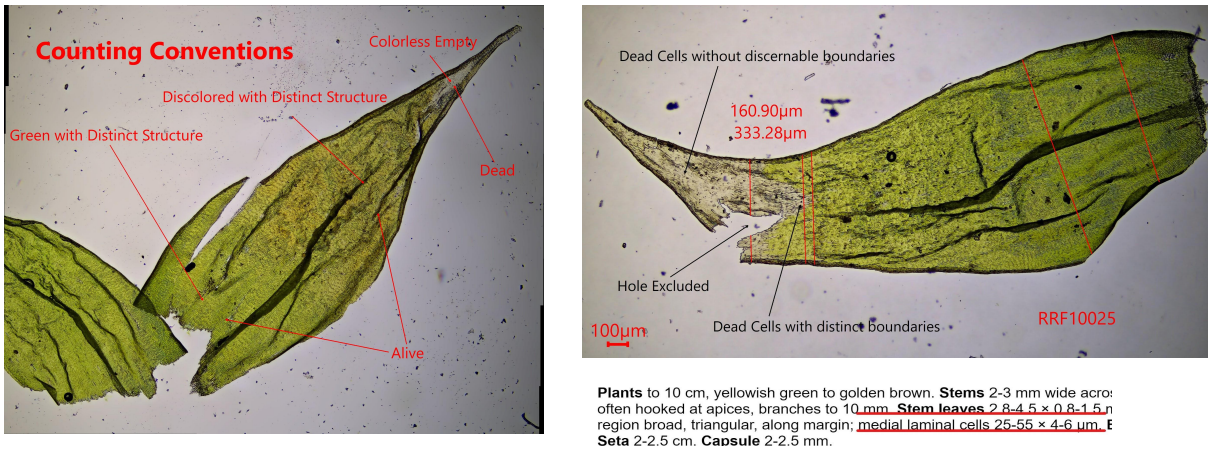

Figure 6: Counting Conventions, Dead Patch, Cell Estimation Source

2.9 Reporting and Analysis:

We computed the mean, median, average, lower quartiles, and upper quartiles for each species in each environment with Matlab. Due to the lack of true replications, we can make no hard and fast claims, but we can provide some insight into what happened.

The scatter plot shown in Figure 7 shows the number of dead cells with increasing distance from the leaf tip. This plot provides a spatial sense of the damage sustained. A linear line of best fit was included to discern any general trends. A positive slope would indicate that damage was generally concentrated towards the base of the leaf while a negative slope would indicate the tip had been damaged.

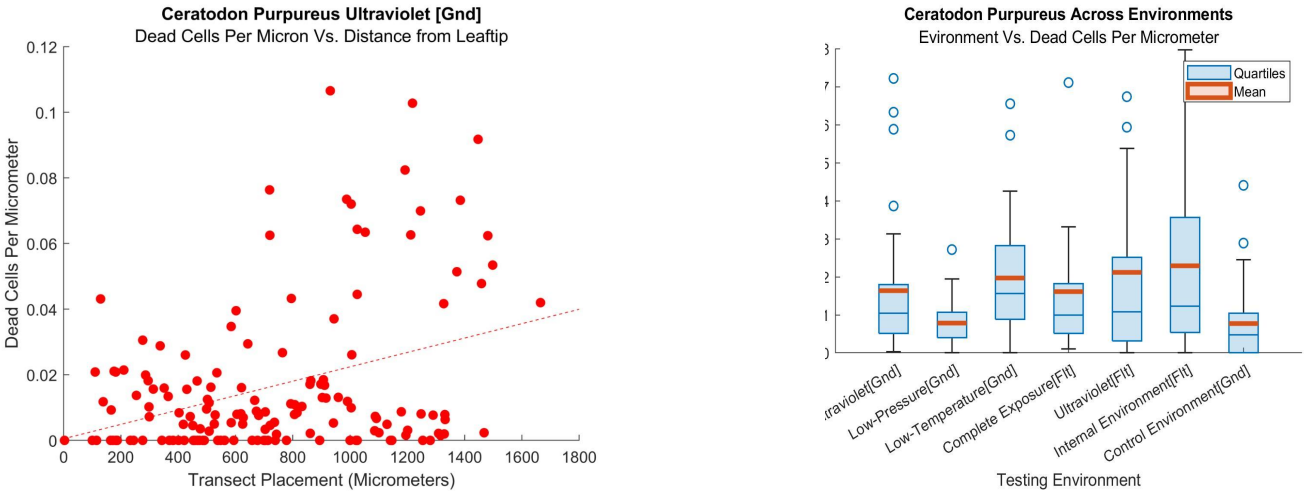

Figure 7: Example Scatter Plot and Box and Whisker Comparison

The box and whisker plot in Figure 7 was used to give a sense of the distribution of data points and put that distribution in context. The y-axis limit was altered to match the greatest maximum value. This is because some extreme outliers scrunched the plots down too far to interpret.

2.10 Testing Plan

(I) Vacuum Test

The samples were contained in a metal cylinder with threads on each end. Vacuum tape and hot glue were used to secure 0.45-micron filter paper to the ends of the cylinder. This measure was taken to ensure that spores did not escape and contaminate other experiments in the chamber. The chamber brought the pressure down to 0.193 Torr over the course of 30 minutes. The pressure was then released over the course of three minutes and the samples were removed and put back in their Petri dishes.

(II) UV Test

A mercury vapor lamp was employed to expose samples to UVA and UVB light. This lamp produced 175 microwatts per square centimeter when placed 15cm away. The lids were removed from the samples and the lamp was hung 15cm above the dishes. The samples were exposed in this manner for 180 minutes. After the time was up, the lids were replaced and the samples returned to the storage area to await microscopy.

(III) Cold Test

Cold testing was carried out using 5lb of dry ice, a styrofoam cooler, a temperature probe, and appropriate gloves. The samples were brought to the target temperature of -30C over the course of 90 minutes. They were then held at that temperature for 30 minutes. When the time was up, the lid of the cooler was removed and the samples were allowed to warm up for another 35 minutes. At that time, the samples were removed from the cooler and returned to the storage area awaiting microscopy.

(IV) Stair Test

The stair test was performed using a set of concrete stairs in a stairwell at the CSU Powerhouse. A metal mass simulator of 240 grams was put in place of the electronics package for the stair and drop tests as there was risk to damage the electronics. Below is a still image from the recording of the stair test.

Figure 8: Stair Test

(V) Drop Test

Next, four drop tests were conducted as it was imperative to mission success that the quartz windows on the payload would not fracture upon landing. If the window were to break this would likely cause the loss of flight samples. The drop tests were conducted by dropping the payload onto cement from around 20 feet. Mass simulators were implemented for these tests as well as they took the place of the mostly completed electronics. Below is a still image from one recording of a drop test.

Figure 9: Drop Test

3.0 Results

3.1 Ground Testing Results

(I) Cold/ Endurance Test

As seen in the bottom right of Figure 10 above, the heating system worked as desired and maintained a cabin temperature between 10 C and 15 C during the payload's exposure to the dry ice. The top left chart represents the temperature of the moss containment above the bay door during the test. It can be seen that this temperature doesn't drop below 5 C before heating up with the rest of the payload. This temperature is survivable for the moss as proven by the ground cold testing of the specimen. Altogether, the cold test was deemed a success due to the ability of the heating system and insulation to maintain the temperatures that were desired.

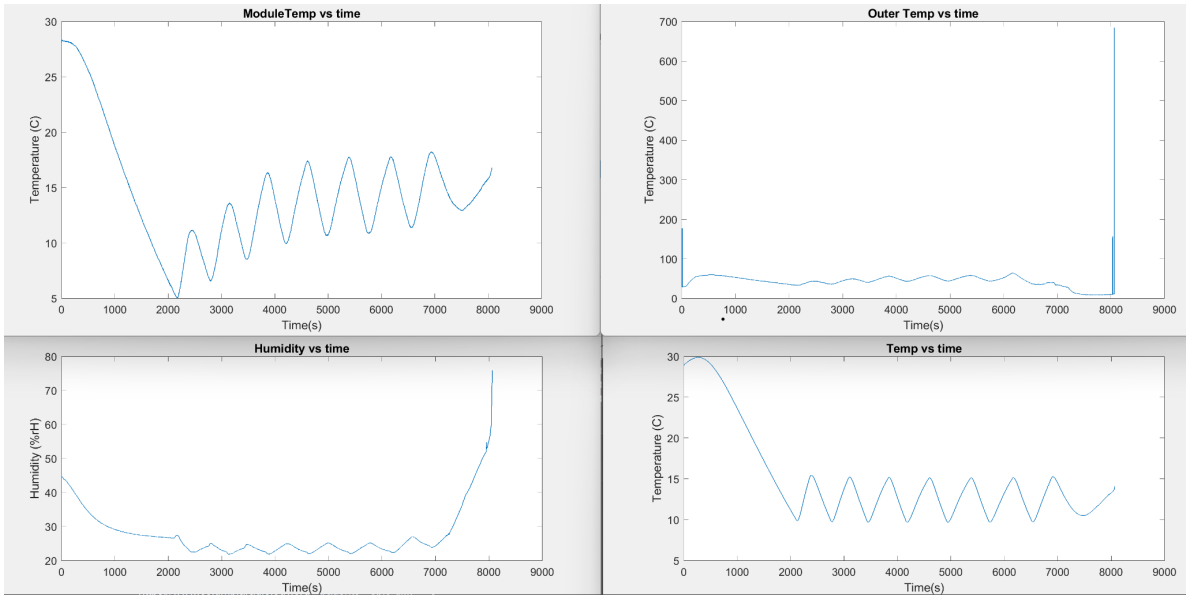

Figure 10: Cold Testing Results

(II) Stair Test

This test simulated the payload landing on the ground and being dragged by the parachute post-flight. The payload remained intact after two iterations of the stair test. This suggested the payload would be able to survive being dragged by the parachute after landing.

(III) Drop Test

The drop tests were deemed successful as the quartz panes didn't break after four consecutive tests. In addition, the main structure remained intact and minimal damage was observed. The bottom side washer, however, did come detached after the fourth drop test. This warranted some redesign of the washer interface to the payload. Altogether, this test provided confidence in the payload's ability to withstand the harsh landing expected upon descent. Another conclusion drawn from this test is that the flight tube was well integrated to the payload as it had landed directly on the protruding flight tube three out of four tests. The flight tube shifted slightly but installed confidence in the design and construction for the flight-ready payload.

(IV) Vacuum Test

Inspecting the samples via microscope revealed that all three species survived the low pressure in significant numbers. *Ceratodon purpureus* showed similar levels of damage as the control sample. *Rhytidium rugosum* also showed similar numbers of dead cells compared to the control sample.

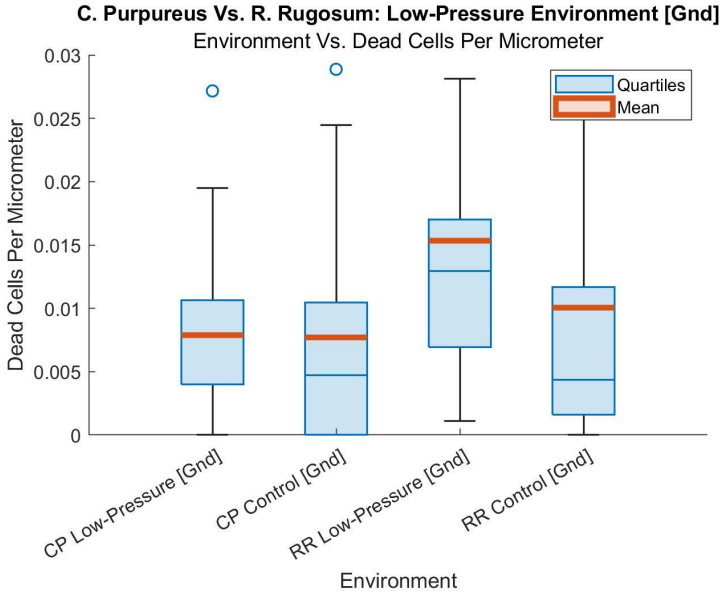

Figure 11: Low-Pressure [Gnd] Box and Whisker Comparison

(V) Cold Test

The cold test samples of *Rhytidium rugosum* showed comparable levels of damage relative to the control with more outliers. However, *R rugosum* had a similar IQR and overall distribution. The samples of *C purpureus* showed an increase in dead cells relative to the control. A sharp spike in humidity was observed during the test.

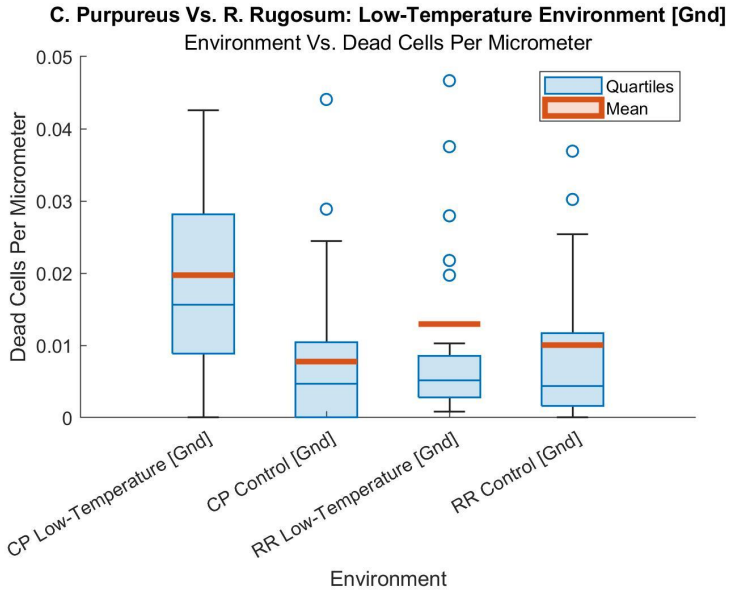

Figure 12: Low-Temperature [Gnd] Box and Whisker Comparison

(VI) UV Test

R rugosum samples showed similar results in the UV test as the control samples. *C purpureus* samples showed nearly identical results in the control and UV tests.

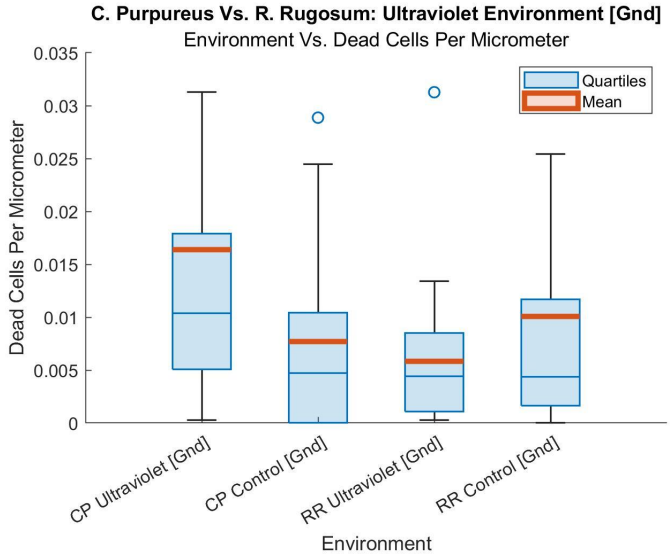

Figure 13: Ultraviolet [Gnd] Box and Whisker Comparison

3.2 Flight Test Results

(I) Payload Operation

The payload operated successfully. The structure survived landing without major damage. The mesh successfully contained the moss stems in the complete exposure environment. The sensor package wrote to the SD card as intended for the entire flight. The bay door opened as intended, though a coding error caused it to open at 10,000m on ascent rather than 500m on descent. The heating system failed to keep the internal environment within the desired temperature range though this may have been caused by the early opening.

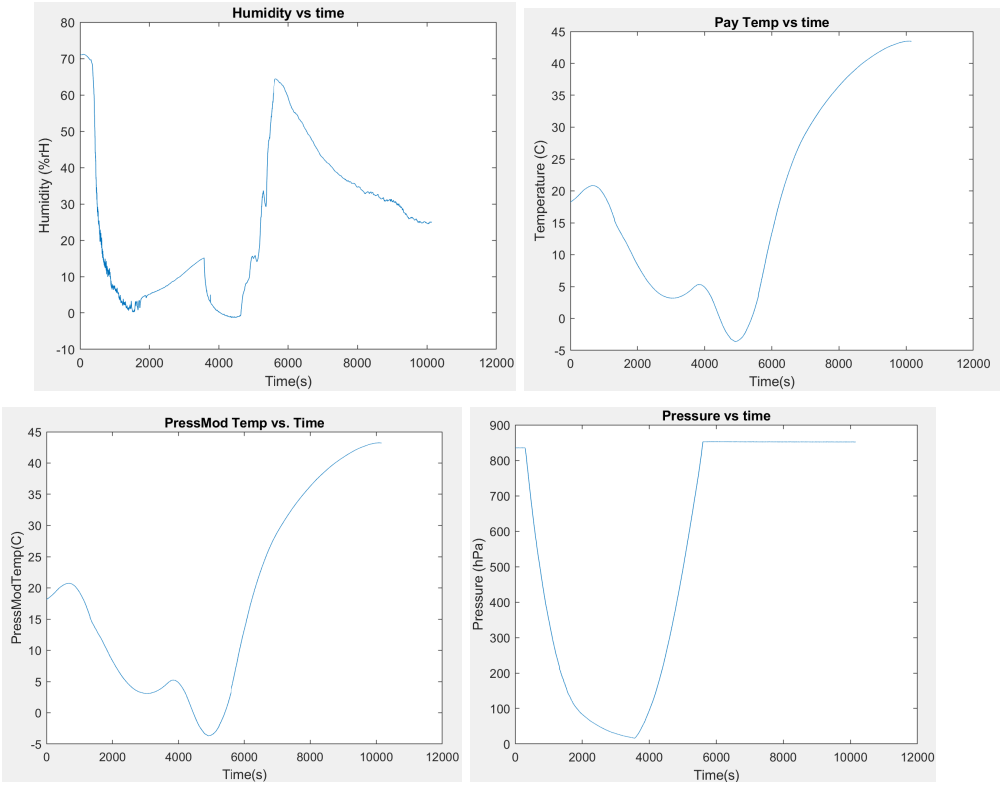

Figure 14: Humidity, Internal Temp (I and II), and Ambient Pressure vs. Time

(II) *Rhytidium rugosum*

The lower quartile, median, upper quartile, and mean values are plotted in Figure 15. The graph shows a bumpy landscape of distributions with the exception of the internal environment which can be seen towering above the rest. Despite the differences in distributions, the mean values across all environments are somewhat comparable.

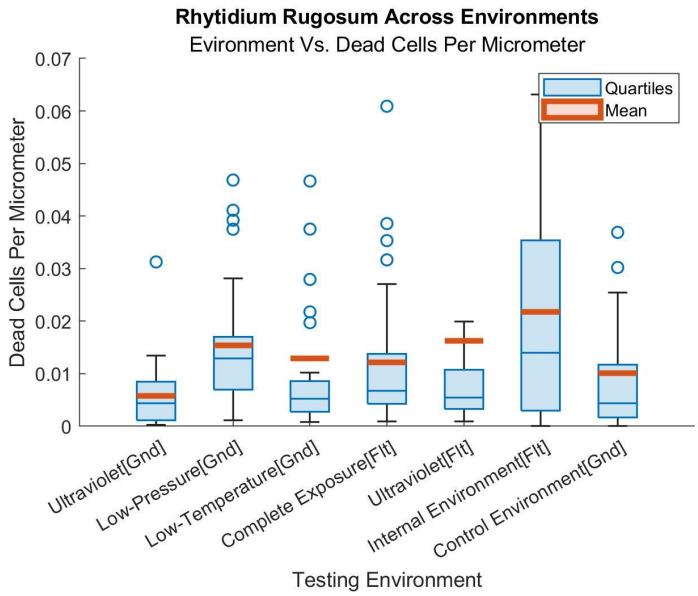

Figure 15: Rhytidium rugosum Box and Whisker Comparison

R. rugosum is a pleurocarpous species meaning that there should not be a significant increase in the number of dead cells as one moves closer to the base. The data collected in the control environment reflect this with only a very gentle slope emerging.

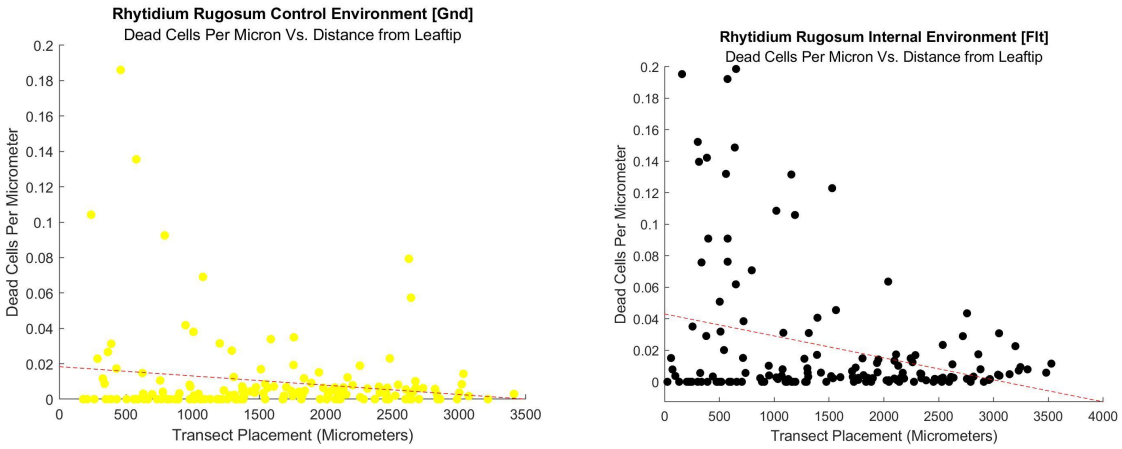

Figure 16: Scatter Plot of R. rugosum in the Control and Internal (F1) Environments

The slope found in the Internal [Flt] environment, shown in Figure 16, is much more pronounced, suggesting that more damage was sustained in the tip of the leaf.

(III) *Ceratodon purpureus*

The average number of dead cells per micrometer for each leaf was calculated using each of the leaf's five transect lines. These values were plotted in Figure 17 as well as the average of those values.

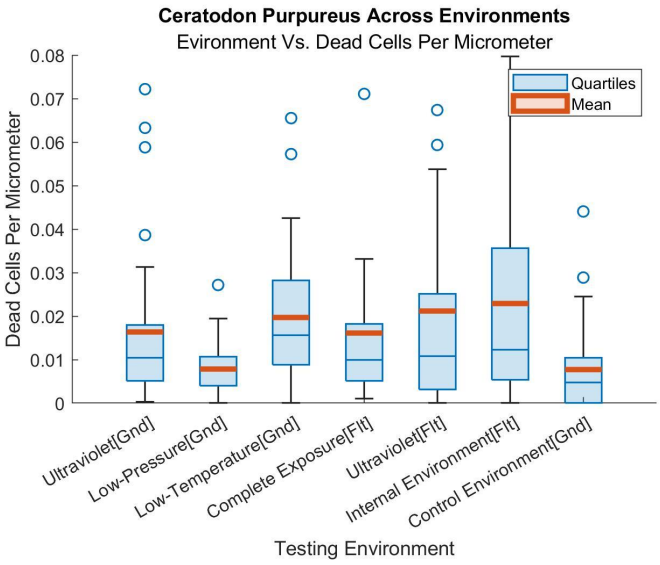

Figure 17: Ceratodon purpureus Box and Whisker Comparison

C. purpureus had the highest average number of dead cells per micron in the Internal, Ultraviolet [flt], and Low-Temperature environments respectively. The Control environment showed the least number of dead cells followed by Low-Pressure and Ultraviolet [Gnd]. The Overall average taken from each of the thirty leaves is shown in Figure 17. Here the contrast between environments is stark. The internal environment showed the greatest number of dead cells. The damage found in the Internal [Flt], Ultraviolet[Flt], and Low-Temperature [Gnd] environments is strikingly similar. There is virtually no difference between the Control [Gnd] and Low-Pressure [Gnd]. The Complete exposure environment [Flt] showed just over twice as many dead cells as the Control environment.

C. purpureus is an acrocarpous species meaning that as the leaf grows its bottommost cells elongate and die. Thus we expected to see a positive trendline in the control sample reflecting this greater number of dead cells towards the base.

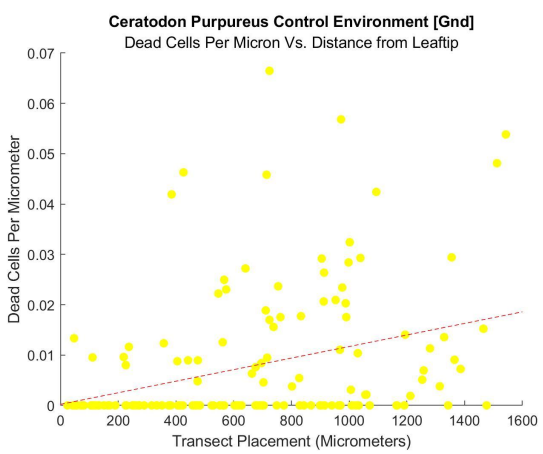

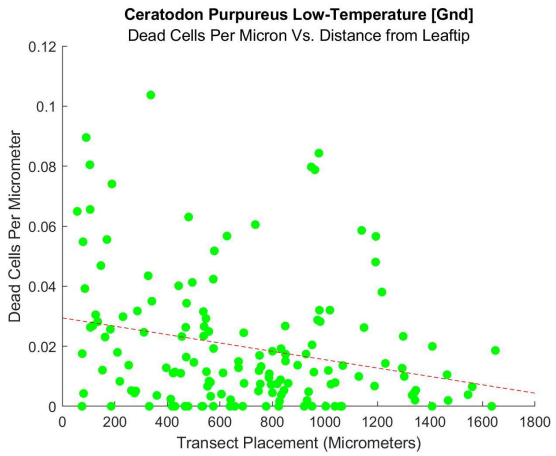

Figure 18: Scatter Plot of C. purpureus in the Control and Low-Temperature Environments

The scatter plot shown in Figure 18 shows the opposite trend in the Low-Temperature [Gnd] environment. This suggests that a disproportionate number of dead cells were found toward the tip.

4.0 Analysis

4.1 Payload

Upon acquiring the payload after launch, the door mechanism opened during the flight and the SD card read data as desired for its duration. After looking at the data it became clear that the door mechanism actuated on the ascent of the payload at an altitude of 10,000 meters. It was desired for the bay door to actuate at 500 meters on its descent. After further investigation, it became apparent that the code had been changed for a small-scale test before launch so that the door would open as one of our team members drove up into the mountains. The code had been written with a less than sign for the door to open as the payload reached an altitude less than 500 meters but was changed to a greater than sign for the pre-launch test. Though the altitudes were changed back after the test, the character wasn't caught to be facing the wrong way, so when the payload reached 10,000 meters, both conditions were automatically met, causing the door to open too early.

```
296
297  if (altitude_delta >= 10000 && y == 1) //Drop Condition
298  {
299    y = 2;
300  }
301
302  if (altitude_delta >= 500 && y == 2)//Door Actuation
303  {
304    //digitalWrite(servo, HIGH);
305    myservo.attach(6);
306    delay(15);
307    myservo.write(20);
308    delay(350);
309    myservo.detach();
```

Figure 19: Code Error

Luckily some insulation was added in case of door failure, yet it wasn't quite enough to keep the whole payload at the desired temperature for the flight. The heating system was set to keep the cabin at a 10-15 degree Celsius range, and is suspected to have worked, but the open door at the peak altitude seemed to be a little too much for the heaters to withstand. The extreme temperatures managed to get the cabin of the payload down to -3.6 degrees Celsius in the flight.

4.2 Moss

We computed the average, median, upper, and lower quartiles. Lacking replications, we did not compute inferential statistical values.

The higher levels of damage C purpureus sustained in the Ultraviolet [Flt], Internal [Flt], and Low-Temperature [Gnd] is likely, not suggestive of a genuine effect. The humidity sensor on board the payload for each of these tests shows that there was a significant increase in humidity in each environment. While we can't say with any certainty, it is possible that this increase in moisture caused the leaves to begin revival prematurely.

The much smaller gaps between the complete exposure environments and control environments suggest that each species of moss would be able to survive exposure to near-space conditions in the dry state and reemerge when rehydrated.

We suggest that further experiments establishing the effects of rehydration in otherwise adverse conditions be conducted.

5.0 Discussion of Error

5.1 Stem Selection:

Ground testing samples were prepared shortly after parent clumps were collected. Flight samples were prepared shortly before launch. By this time the clumps were dryer and more brittle. For Ground testing, RR stems were taken whole including all of the offshoot stems. The offshoot stems have shorter leaves that are a slightly different shape. For flight testing, only the main stems were taken for testing. This ensured that leaves were all the largest and all the same kind.

5.2 Leaf Selection:

Due to the nature of moss species, leaves towards the base of a stem die as the stem grows upwards. If any of the leaves imaged were from the lower part of the stems this would throw off the number of dead cells significantly. We tried to take leaves as far up the stem as possible. The very tip of the stem was excluded as these leaves were young and immature.

Dead leaves are more brittle and easier to break and tear while handling. It was more difficult to get such leaves under a microscope intact enough to image. It is possible that less damaged leaves were imaged disproportionately as they were easier to dissect.

5.3 Ground Testing

There was a significant difference in air temperature between the flight and the low-temperature test. The amount of UV light that samples were exposed to in ground testing was not connected to the amount experienced in flight.

5.4 Cell Counting

The method of counting was not consistent across testing environments. All the counting for CP in ground testing, including CPUV, CPLP, CPLT, and CPCT were all counted by one experimenter. RRUV, RRLP, and RRLT were all counted by different experimenters. The comparison between these environments is very tenuous as a result. This issue was identified and each experimenter counted one-third of the leaves for each species in each environment for flight testing.

5.5 Confounding Variables

Since the test was not replicated and the samples were not randomly distributed in their environments the presence of confounding variables cannot be eliminated.

In cold testing, it was observed that the humidity within the payload jumped significantly. The same was observed in flight. The UV Exposure and Internal Environment containment mechanisms were sealed. It is possible that humidity increased in these compartments during flight causing premature revival.

5.6 Sensor Accuracy:

While all payload sensors read data throughout the flight, many of the values proved inaccurate. This conclusion was reached following comparisons between payload sensors and those provided by EOSS. The outside temperature and pressure values were somewhat different.

6.0 Conclusions

6.1 Payload

The functioning sensor package, heating system, and door mechanism demonstrate that this design is capable of exposing moss samples to three distinct environments and releasing moss samples at low altitudes.

6.2 Moss

The data collected suggest that both *R. rugosum* and *C. purpureus* can revive after enduring near-space conditions. The higher death rate in sealed containers suggests humidity may exacerbate damage in extreme conditions. Short-term UV radiation is likely unimportant.

7.0 Message To Next Year

Our message for next year is to ask questions early and ask them often. Communication is key and can aid greatly in avoiding issues later in the project. Also, make sure you schedule to finish your project at least two weeks before the deadline. This gives a nice cushion so that if there are unforeseen issues, they can be addressed properly and there is no rushing. Altogether,

make sure that you pick something that will be of interest to you, think ahead about every possibility and the consequences of those possibilities, and measure twice and cut once.

Appendix

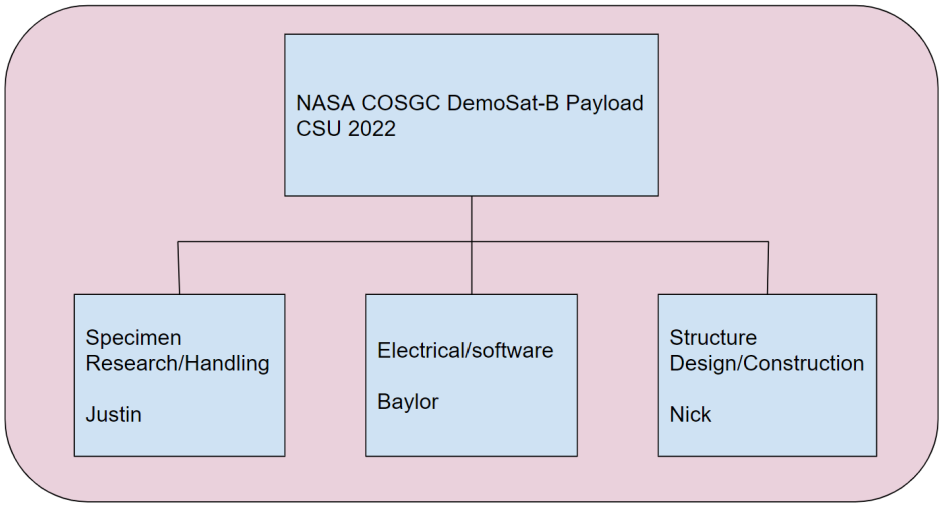

Figure 20: Project Organization Chart

Items (Pre-Build Weights)	Weight per unit (g)	Quantity	Subtotal (g)
Arduino MEGA Shield	22	1	22
7.4V Li-po Battery	81	2	162
SD Card Module + SD	5	1	5
GPS Mod + Antenna	16	1	16
K-Type Thermocouple + Module	14	1	14
Arduino MEGA 2560	36	1	36
Real Time Clock	7	1	7
Stepper Motor Driver	7	1	7
Stepper Motor	32	1	32
Servo Motor	10	1	10
UV Sensor	3	1	3
Atm Breakout	3	1	3
Relay Module	14	1	14
Mounting Plates + Fasteners	60	1	60
Quartz UV Grade	6	4	24
Dispersion Guides and Grid	42	1	42
Dispersion Door	8	1	8
Spool	3	1	3
UV Specimen Containment	10	1	10
Contrl Specimen Containment	10	1	10
Mesh	4	1	4
Control Containment	12	1	12
Washer	10	2	20
Flight Tube	16	1	16
Structure/Insulation	350	1	350
Wiring	22	1	22
Heating System (and circuit)	48	1	48
Switch	3	1	3
Zipties	0.5	10	10
		Total	973
		Actual Total	990

Table 2: Weight Budget

Item	Price per unit	Quantity	Subtotal	Vendor
7.4V Li-po Battery	$26.99	1	$26.99	Amazon
SD Card Module + SD	$5.99	1	$5.99	Amazon
GPS Mod + Antenna	$12.99	1	$12.99	Amazon
K-Type thermocouple	$13.99	1	$13.99	Amazon
Arduino MEGA 2560	$38.10	1	$38.10	Amazon
UV Sensor	$11.95	1	$11.95	SparkFun
Atm Breakout	$29.95	1	$29.95	SparkFun
Relay Module	$6.79	1	$6.79	Amazon
Quartz UV Grade	$42.00	2	$84.00	Amazon
PETG Filament	$15.99	1	$15.99	Amazon
UV Bulb	$48.95	1	$48.95	Amazon
UV Light Power Cord	$10.99	1	$10.99	Amazon
MAX31855	$17.13	1	$17.13	Amazon
Mesh Sheets	$8.99	1	$8.99	Amazon
Filter Paper	$23.99	1	$23.99	Amazon
Plugs for UV lights	$10.99	1	$10.99	Amazon
Microscope slides + covers	$8.99	1	$8.99	Amazon
Petri Dishes	$13.99	1	$13.99	Amazon
Winter Radish Seeds	$5.99	3	$17.97	Amazon
Heating Pads	$5.50	1	$5.50	SparkFun
MS5803 Altimeter	$64.50	1	$64.50	Sparkfun
Thermister	$6.00	1	$6.00	Amazon
GPS Antenna Extension	$7.70	1	$7.70	Amazon
Real Time Clock	$0.00	1	$0.00	Donated
Stepper Motor Driver	$0.00	1	$0.00	Donated
Stepper Motor	$0.00	1	$0.00	Donated
Washer	$0.00	2	$0.00	Donated
Flight Tube	$0.00	1	$0.00	Donated
Aluminum Tape	$0.00	1	$0.00	Donated
Plastic Mounting Plates	$0.00	1	$0.00	Donated
Insulation	$0.00	1	$0.00	Donated
Shipping and Handling	$50.00	1	$50.00	
		Total	$542.43	
		With 10% margin	$596.67	

Table 3: Total Expenses

Works Cited:

A. Andrio, “International Symposium on Bioremediation, Biomaterial, Revegetation, and Conservation,” in *Development of UAV Technology in Seed Dropping for Aerial Revegetation practices in Indonesia*, vol. 308, pp. 1–6.

A. Post, “Photoprotective pigment as an adaptive strategy in the Antarctic Moss ceratodon purpureus,” *Polar Biology*, vol. 10, no. 4, pp. 241–246, 1990.

B. Asher, “Describe the structure of a moss plant,” *Sciencing*, 18-Nov-2019. [Online]. Available: https://sciencing.com/describe-the-structure-of-a-moss-plant-12000232.html. [Accessed: 17-Jun-2022].

B. Clément and J. Touffet, “Vegetation Dynamics in Brittany Heathlands after fire,” *Vegetation dynamics in grasslands, heathlands and mediterranean ligneous formations*, vol. 46, pp. 157–166, 1981.

B. Fernández-Marín, I. Kranner, M. S. Sebastián, U. Artetxe, J. M. Laza, J. L. Vilas, H. W. Pritchard, J. Nadajaran, F. Míguez, J. M. Becerril, and J. I. García-Plazaola, “Evidence for the absence of enzymatic reactions in the glassy state. A case study of xanthophyll cycle pigments in the desiccation-tolerant Moss Syntrichia ruralis,” *Journal of Experimental Botany*, vol. 64, no. 10, pp. 3033–3043, Jun. 2013.

B. Winter, “A Very Basic Tutorial for Performing Linear Mixed Effect Analyses,” pp. 2–18, 2013.

H. Lepp, “Sexual vs. Vegetative: Reproduction and Dispersal,” *Australian Bryophytes*, 28-Feb-2008. [Online]. Available: https://www.anbg.gov.au/bryophyte/sexual-vegetative.html. [Accessed: 12-Aug-2022].

J. Burch, “Some Mosses Survive Cryopreservation without Prior Treatment,” *The Byrologist*, vol. 106, no. 2, pp. 270–277, 2003.

J. M. Graham, “American Institute of Physics Conference Proceedings,” in *Stages in the Terraforming of Mars: The Transition to Flowering Plants*, 2003, pp. 1284–1291.

J. R. Rohrer, “Rhytidium,” *Flora of North America North of Mexico*, vol. 28, p. 339, 2014.

J. Royles, J. Ogée, L. Wingate, D. A. Hodgson, P. Convey, and H. Griffiths, “Temporal Separation between CO 2 Assimilation and Growth. Experimental and Theoretical Evidence from the Desiccation tolerant moss Syntrichia Ruralis.,” *New Phytologist*, vol. 197, no. 4, pp. 1152–1160, 2013.

K. A. Platt, M. J. Oliver, and W. W. Thomson, “Membranes and organelles of dehydrated selaginella and Tortula retain their normal configuration and structural integrity,” *Protoplasma*, vol. 178, no. 1-2, pp. 57–65, 1994.

K. L. Koster, R. A. Balsamo, C. Espinoza, and M. J. Oliver, “Desiccation sensitivity and tolerance in the Moss Physcomitrella Patens: Assessing limits and damage,” *Plant Growth Regulation*, vol. 62, no. 3, pp. 293–302, Jun. 2010.

M. Arroniz-Crespo, D. Gwynn-Jones, T. V. Callaghan, E. Nunez-Olivera, J. Martinez-Abaigar, P. Horton, and G. K. Phoenix, “Impacts of long-term enhanced UV-B radiation on bryophytes in two sub-arctic heathland sites of contrasting water availability,” *Annals of Botany*, vol. 108, no. 3, pp. 557–565, 2011.

M. J. Oliver, Z. Tuba, and B. D. Mishler, “The Evolution of Vegetative Desiccation Tolerance in Land Plants,” *Plant Ecology*, vol. 151, pp. 85–100, 2000.

M. T. Gallego, M. J. Cano, R. M. Ros, and J. Guerra, “An overview of Syntrichia ruralis complex (pottiaceae: Musci) in the Mediterranean region and neighbouring areas,” *Botanical Journal of the Linnean Society*, vol. 138, no. 2, pp. 209–224, Jul. 2002.

N. Ghandi, K. Rahul, N. Chandana, B. Madhuri, and D. Mahesh, “Impact of Ultraviolet Radiation on seed germination, growth and physiological response of Bengal gram (Cicer arientum L.) and Horse Gram (Macrotyloma uniflorum L.),” *Journal of Biochemistry Research*, vol. 2, no. 1, pp. 19–34, 2019.

R. E. Longton, “Role of bryophytes and lichens in terrestrial ecosystems - ESF | SUNY ESF,” *College of Environmental Science and Forestry*, 1992. [Online]. Available: https://www.esf.edu/efb/Kimmerer/mossecology/reserve/Role_of_bryophytes_and_lichens_in_terrestrial_ecosystems.pdf. [Accessed: 26-May-2022].

R. E. Noble, “Effects of UV-irradiation on seed germination,” *Science of The Total Environment*, vol. 299, no. 1-3, pp. 173–176, May 2002.

R. Lemmons, “Specific effects of UVB radiation on plants - ultraviolet radiation,” *Climate Policy Watcher*, 03-Apr-2022. [Online]. Available: https://www.climate-policy-watcher.org/ultraviolet-radiation-2/specific-effects-of-uvb-radiation-on-plants.html#:~:text=Plants%20are%20highly%20sensitive%20to,(DNA)%20within%20the%20nucleus. [Accessed: 26-May-2022].

S. Dołęgowska and Z. M. Migaszewski, “Plant sampling uncertainty: A critical review based on Moss Studies,” *Environmental Reviews*, vol. 23, no. 2, pp. 151–160, Jan. 2015.

S. Lett, L. M. Teuber, E. J. Krab, A. Michelsen, J. Olofsson, M. C. Nilsson, D. A. Wardle, and E. Dorrepaal, “Mosses modify effects of warmer and wetter conditions on tree seedlings at the Alpine treeline,” *Global Change Biology*, vol. 26, no. 10, pp. 5754–5766, 2020.

Takashima-Oliveira, Tássia T G et al. “Bryophyte communities across the ecological succession process in the Caxiuanã National Forest, Pará, Brazil.” *Anais da Academia Brasileira de Ciencias* vol. 92,1 e20180626. 9 Apr. 2020, doi:10.1590/0001-3765202020180626

Y. Takahashi, H. Hashimoto, T. Nakagawa, and S. Shibata, “Survivability of moss and fungal spores in tests simulating conditions of the ISS Outer Wall,” *Biological Sciences in Space*, vol. 25, no. 2_4, pp. 83–92, 2011.